Evolution of ferromagneticlike order in $Fe_2V_{1-x}Cr_xAl$ Heusler alloys

Ritwik Saha and V. Srinivas*
Department of Physics and Meteorology, Indian Institute of Technology Kharagpur, Kharagpur 721302, India

T. V. Chandrasekhar Rao
Technical Physics and Prototype Engineering Division, Bhabha Atomic Research Centre, Mumbai 400085, India
(Received 30 January 2009; revised manuscript received 20 April 2009; published 18 May 2009)

Structural, magnetic, and magnetotransport behaviors of $Fe_2V_{1-x}Cr_xAl$ Heusler-type alloys have been investigated in the present work. From the detailed analysis of data it is observed that increasing Cr content promotes site disorder of Fe and Al, which in turn leads to destabilization of $L2_1$ superstructure of Fe_2VAl. This site disorder seems to enhance the magnetic moment through spatially confined magnetic entities and intercluster interactions, transforming the alloy system into a magnetically ordered state in the limit $x \rightarrow 1$. Low-temperature magnetoresistance (MR) values drop quite rapidly from $\sim 10\%$ for $x=0$ to 0.4% for $x=0.8$, suggesting that magnetic interactions have a role in MR deterioration. Further the MR exhibits a maximum at a particular temperature in the vicinity of magnetic transition temperature, where interaction effects weaken. Our magnetization data support MR results and suggest that undoped Fe_2VAl exhibits cluster-glass behavior with optimum superparamagnetic (SPM) contribution, developed possibly due to the random anisotropy with the presence of V. However, in Cr-substituted alloys anisotropy reduces due to coupling between the clusters, which, in turn, results in reduced SPM contribution and low MR values.

DOI: 10.1103/PhysRevB.79.174423 PACS number(s): 75.10.−b, 72.15.Gd, 36.40.Cg, 61.66.Dk

I. INTRODUCTION

The term Heusler alloys refers to a large family of intermetallic compounds, which attract considerable attention due to a variety of physical properties that they exhibit. Although these alloys have been actively investigated for more than three decades, there are still uncertainties in basic understanding. A renewed interest on Heusler-type intermetallic alloys has been triggered by the prediction of half metallicity.[1] The main feature of the electronic structure of half-metallic materials is the presence of an energy gap at the Fermi level in one of the spin subbands and metallic character of the density of states (DOS) in the other subband,[1–3] which leads to 100% spin polarization of charge carriers. This feature can result in unusual electronic properties that are suitable for novel spintronic applications. Such materials are also attractive from the perspective of both fundamental physics as well as industrial applications, as they exhibit a range of magnetic and electrical properties with features reminiscent of magnetic semiconductors. The ternary intermetallic Heusler alloys represented by the general formula X_2YZ exhibit $L2_1$ crystal structure, where X and Y are transition metals and Z is often an element with sp-type valence electrons from III-VI groups in periodic table. Among various Heusler compositions, considerable attention has recently been paid to Fe_2TMAl (TM: $3d$ transition metals such as V, Cr, and Ti) as significant changes in the electronic band structure have been observed near the Fermi level.[4] Rather puzzling electronic properties were reported in Fe_2VAl system and related compositions.[5] For example, it exhibits nonmetallic character despite being constituted by metallic elements and is reported to be nonmagnetic down to 2 K (Ref. 5) despite half of its atoms being iron. On the other hand Fe_2TiAl shows electrical and optical properties that are reported to be typical of metals, but is weakly magnetic.[3,4] These reports suggest that nonmetallic behavior could be triggered by magnetic disorder in the isostructural Fe_2TMAl (TM: V, Cr) compounds. It is interesting to point out that these compounds belong to an alloy system wherein the TM/Fe ratio can be varied continuously to investigate the role of structural/chemical disorder on electronic and magnetic properties. Slebarski *et al.*[6] investigated electronic properties of isostructural $Fe_2V_{1-x}Ti_xAl$ ($x=0-1$) and found that the reduction in electron density alters both nonmetallic and magnetic behaviors of Fe_2VAl alloy. Further they suggested that a critical composition $x=0.1$ separates the nonmagnetic compounds with a hybridization gap from the other magnetic metals ($x \geq 0.3$). It is now well established from various experimental investigations as well as theoretical calculations that the electronic properties are sensitive to elemental substitution as well as the stoichiometric limit of an ideal Heusler ($L2_1$) structure.[7–13] This structure is based on an underlying bcc lattice of lattice constant $a/2$, with TM at (0,0,0), Al at (1/2,1/2,1/2) a, and Fe atoms at (1/4,1/4,1/4) a and (3/4,3/4,3/4) a, where a is the lattice constant of resulting fcc compound. The $L2_1$ structure consists of four interpenetrating fcc planes A, B, C, and D. A and C sublattices are equivalent and are occupied by Fe atoms, sublattice B by TM atoms, and sublattice D by Al atoms as opposed to TM and Fe randomly entering the A, C, and B sites in B2 crystal structure. Besides, $L2_1$ structure is similar to that of Fe_3Al, which has two inequivalent Fe sites: Fe_I site (which is the TM site in Fe_2TMAl) has eight Fe neighbors in octahedral configuration, while Fe_{II} site has four Fe and four Al neighbors. All transition-metal atoms that lie to the left of Fe in the periodic table (TM=Cr, V, Ti) follow this trend.[4]

Irrespective of constituents present in most Heusler-type alloys, the chances of a disordered structure being formed are significant. In particular the iron-based TM alloys show a great sensitivity to environmental effects. Indeed the electronic properties of Fe_2VAl composition are very sensitive to the substitution of elements, disorder, and processing

parameters.[14,15] On the theoretical front, first-principles calculations on a perfectly ordered structure show a deep pseudogap in DOS near the Fermi level[11]—a result later confirmed through experiments on Fe_2VAl system. However, if structural disorder or site disorder is incorporated into such calculations additional states may emerge in the pseudogap region of energy-band spectrum of Fe_2VAl alloy that can affect its physical properties. Indeed a significant decrease in resistivity, magnetization, and magnetoresistance values has been reported with quenched disorder.[16–18] Slebarky *et al.*[19] suggested that a weak ferromagnetic and heavy fermion behavior could be induced in Heusler alloys due to atomic disorder. When atoms of another *d* metal replace vanadium atoms, the Fermi level remains within the pseudogap in one spin subband and is in the region of a high DOS in the other subband. Thus the replacement of V atom leads to the formation of a state with a high spin polarization of electrons in the alloys, which is close to the half-metallic ferromagnetic state. With this viewpoint electronic properties of Fe_2TiAl system have been investigated but they appear to be more complex probably due to the presence of small amount of secondary Fe_2Ti phase in C_{14} structure. Band-structure calculations predicted Fe_2TiAl to exhibit anomalous electronic properties, but experimentally it was found to be metallic with a magnetic transition around 100 K.[20] On the other hand, Fe_2CrAl stabilizes in single phase B2-type crystal structure possessing nonmetallic but ferromagnetic behavior with Curie temperature (T_C) of 246 K.[20,21] Contrary to these observations coexistence of paramagnetic and weak ferromagnetic components in the temperature range of 40–296 K has also been reported.[22] It was also observed that magnetic transition extends over a wider temperature range (T_C =330), disappearing with increasing magnetic field intensity, attributed to the clustering of Cr atoms,[22,23] formation of Fe clusters,[4] or presence of Cr clusters around Fe.[24] Although from electronic structure calculations Fe_2CrAl system was predicted to be a half-metallic ferromagnet[25] (HMF) the experimental results showed nonmetallic character with higher density states at the Fermi level compared to Fe_2VAl.[4,20] However, significant changes observed in the magnetic behavior were attributed to the magnetic cluster size and density variations.[16,17] In another study Vasundhara *et al.*[18] suggested a magnetic cluster-glass state in Fe_2VAl with clusters of different sizes. In the literature it is suggested that substitution of Cr in Fe_2VAl can lead to half-metallic ferromagnetic behavior.[20] To the best of our knowledge, such studies have not been carried out till now and we were motivated to investigate how a nonmagnetic semiconducting alloy such as Fe_2VAl transforms into ferromagnetic semiconducting Fe_2CrAl. Besides, we intend to understand why and how the ferromagnetic character gets suppressed in Fe_2VAl alloy system.

Magnetoresistance (MR), on the other hand, is intrinsically connected with the electron mean-free path, i.e., a range of a few nanometers. The large MR values observed in magnetically heterogeneous system are satisfactorily explained on the basis of the spin dependent scattering of the electrons.[26] For example, the magnetization and magnetic transport properties of granular alloy (consisting superparamagnetic particles embedded into metallic nonmagnetic matrix) have been extensively studied.[26–28] In such systems, simultaneous presence of nonsaturating magnetic behavior up to very large applied magnetic fields and steep magnetization changes at lower fields are seen due to the particle size dispersion, along with irreversible effects in temperature-dependent magnetization. From the Monte Carlo simulations, it was shown that magnetic cluster size dispersion alone causes enhancement of MR, while the interactions always have a degrading effect. Most interestingly, the effect of dipolar interactions is amplified in the presence of a wide distribution of cluster sizes. Therefore, it is suggested that normalized MR curves provide an indication of the relative importance of the interaction effects. Thus, magnetization and magnetotransport measurements provide complementary information from which one can obtain an unambiguous picture about the magnetic state of the sample in question. Therefore a comparative study of magnetic and magnetotransport properties of Cr substituted Fe_2VAl alloys, with same process conditions and method of preparation can provide valuable information on the nature of magnetic interactions present in these alloys.

In this paper we report on structural, magnetic, and magnetoresistance behaviors in Cr-substituted Fe_2VAl alloys synthesized under same processing conditions in order to address the following issues: (i) while Heusler-type compositions Fe_2VAl and Fe_2CrAl stabilize in two different crystal structures, they exhibit similar electrical characteristics and contrasting magnetic behavior, (ii) the critical composition at which the structural transition takes place, in order to unravel the effect of site disorder on physical properties, (iii) whether the magnetic transition observed in Fe_2CrAl is a true FM→PM transition or a glassy state, and (iv) whether any correlation exists between magnetic properties and magnetotransport behavior of the system.

II. EXPERIMENTAL DETAILS

The alloy ingots of $Fe_2V_{1-x}Cr_xAl$ (x=0, 0.2, 0.4, 0.6, 0.8) were prepared with high-purity elemental constituents using an arc-melting furnace under argon atmosphere. Melting was carried out several times in order to homogenize the samples. The ingots were then sealed in evacuated quartz tubes and annealed at 950 °C for 72 h. The nominal composition assigned to each sample is regarded as accurate, since the weight loss was found to be 0.3%–0.5%. Further the elemental analysis was carried out using an energy dispersive x-ray analyzer attached with scanning electron microscope Model Supra 40 of Carl Zeiss SMT Ltd with 5 kV operating voltage. The analytical values are in agreement with the nominal compositions reported in this study. Ingots were then cut into suitable shapes ($2\times3\times5$ mm^3) using spark-erosion technique for the physical property measurements. The crystallographic structure was identified using powder x-ray diffraction (XRD) patterns taken with Cu K_α radiation of wavelength λ=0.154 18 nm using a P.W. 1718 x-ray diffractometer. Magnetization data as a function of applied fields up to 15 kOe and temperatures down to 7 K were recorded using a commercial superconducting quantum interference device (SQUID) magnetometer (Quantum Design, MPMS).

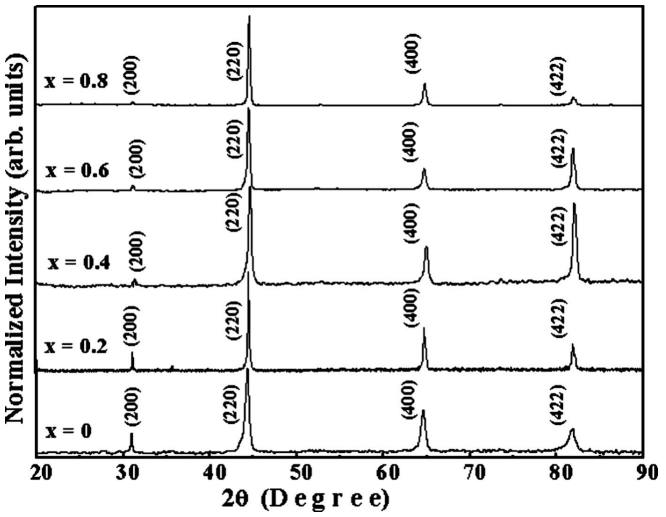

FIG. 1. X-ray diffraction patterns (Normalized Intensity) of $Fe_2V_{1-x}Cr_xAl$ (x=0–0.8) alloys.

Magnetoresistance measurements as a function of temperature (5–300 K) and applied magnetic field (0–50 kOe) have been carried out using conventional four-probe technique in a cryogen free superconducting magnet system (5TL-VRTB30, Janis Research Co., USA).

III. RESULTS AND DISCUSSION

A. X-ray diffraction

The x-ray diffraction patterns of the $Fe_2V_{1-x}Cr_xAl$ ($0 \leq x \leq 1$) alloys were identified to be of single phasic materials with cubic structure. As shown in Fig. 1, the presence of strong reflections at (200), (220), (400), and (422) in XRD patterns confirms the expected $L2_1$ crystal structure with $Fm3m$ space group with no sign of the presence of secondary phases. The lattice parameter essentially remains constant, confirming that Cr occupies V atomic sites according to Vegard's law, as there is no significant difference between the ionic radii of Cr and V. The overall XRD pattern remains same on V replacement by Cr. However, on close examination, one can observe that the intensity of (200) diffraction peak gradually decreases as Cr concentration is increased in the solid solution $Fe_2V_{1-x}Cr_xAl$. The x-ray intensities of the lines are given by

$$I_{111} \sim [(f_a - f_b)^2 + (f_c - f_d)^2],$$

$$I_{200} \sim [f_a - f_b + f_c - f_d]^2,$$

$$I_{220} \sim [f_a + f_b + f_c + f_d]^2,$$

where f_a, f_b, f_c, and f_d are the average scattering factors for the atoms in the respective sublattices. Moreover we have found a distinct influence of the Cr content on the intensity ratio between the even superlattice reflections (200) and (220), i.e., I_{200}/I_{220}. The value of the I_{200}/I_{220} decreases with increasing x from 24% for x=0 to 5% for x=0.8 Since the ratio I_{200}/I_{220} is a measure of the degree of site ordering of Fe and Al atoms, we can conclude that enhanced incorporation of Cr into the lattice promotes a reduction of the site ordering (i.e., site occupancy is increasingly randomized), as all the alloys have been prepared and processed under identical conditions. Since site disorder plays a significant role in altering the magnetic and electrical transport properties of Heusler compositions, in depth magnetic and magnetotransport measurements have been carried out and discussed below.

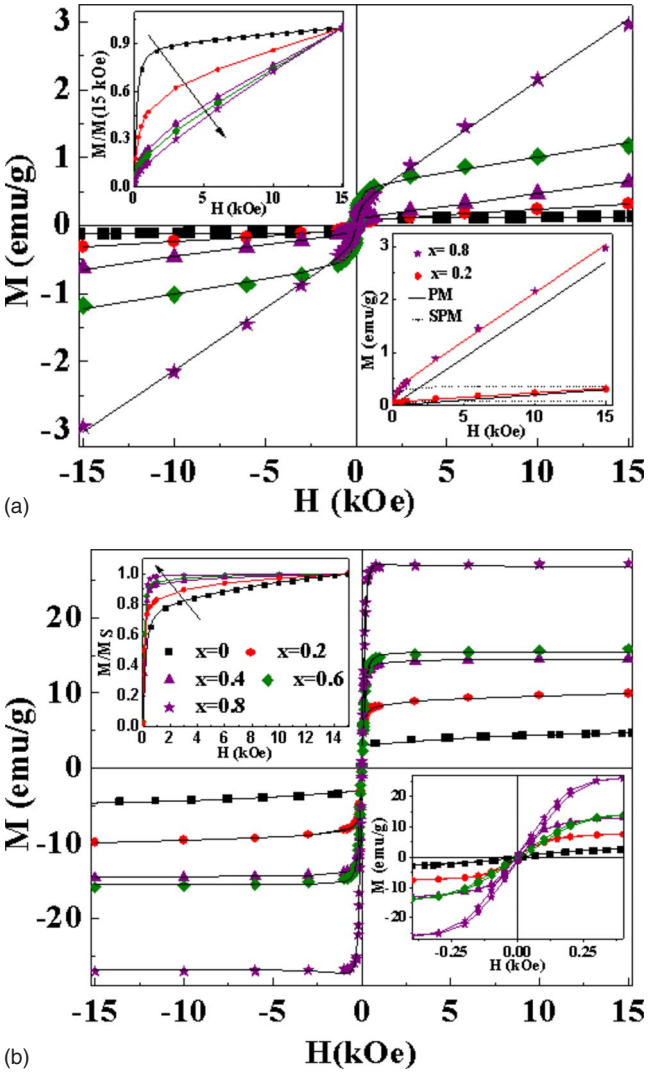

FIG. 2. (Color online) (a) (Main panel) M-H hysteresis loops for $Fe_2V_{1-x}Cr_xAl$ at 300 K. Insets: (upper) Normalized magnetization as a function of H. (lower) Separated SPM and PM components of x=0.2 and 0.8 from the fits to Eq. (1). Symbols used in (a) and (b) represent same composition. Legend is given in (b). (b) (Main panel) M-H hysteresis loops for $Fe_2V_{1-x}Cr_xAl$ at 7 K. Insets: (upper) Normalized magnetization as a function of H. (lower) Low-field hysteresis loops for better view of magnetic parameters. Solid lines through the data points represent fits to the Eq. (3).

B. Field dependence of magnetization

The variation of magnetization (M) as a function of applied field (H) for all the samples is shown in Figs. 2(a) and

2(b) at temperatures 300 and 7 K respectively. The magnetization curves at 300 K display (i) low M values for $x=0$, (ii) increase in M with increasing Cr concentration but no saturation even at applied magnetic fields of 15 kOe, (iii) a sharp rise in M at low fields for lower Cr content alloys and a dominant linear component for high Cr content alloys [see top inset of Fig. 2(a)], and (iv) negligibly small remnant magnetization (M_R) and coercivity (H_C) values. The absence of hysteresis and spontaneous magnetization (M_S), as well as the approach to the saturation are a good indication of presence of two magnetic components in low Cr content alloys. It is evident from Fig. 2(a) (top inset) that $x=0$ sample shows a rapid increase in M at low fields and a tendency for saturation (with low values of M) while for $x=0.8$ sample M is linear at higher H. These observations suggest that even at 300 K ferromagnetic correlations exist in $x=0$ and they get suppressed as x is increased. The nonlinear M-H curve of $x=0.8$ also suggests the presence of a dominant para- or antiferromagnetic (AFM) component, coexisting with a weak ferromagnetic (FM) state. These results cannot be explained on the basis of conventional theories. Therefore an analytical expression with a combination of two magnetic components has been employed to identify the magnetic interactions. Among various combinations of magnetic contributions, the experimental curves at 300 K could be well described by assuming a combination of superparamagnetic (SPM) and paramagnetic (PM) components, with a minimum number of fitting parameters, using a modified Langevin function represented by

$$M(H) = M_S L(\alpha) + \chi_f H, \tag{1}$$

where $L(\alpha)=[\mathrm{Cos}(\alpha)-1/\alpha]$, with $\alpha=\mu H/k_B T$ is the Langevin function, M_S is the saturation magnetization, μ is the average magnetic moment per cluster, and χ_f is the field-forced susceptibility associated with intrinsic magnetization. The fits to Eq. (1) and the resulting SPM and PM components are shown for $x=0.2$ and 0.8 samples in the bottom inset of Fig. 2(a). From these fits magnetic cluster moment is obtained to be $5517\mu_B$ for $x=0$, decreasing to $2595\mu_B$ for $x=0.8$. Thus PM component progressively increases with increasing Cr content which is reflected in χ_f variation from $\sim 10^{-5}$ for $x=0$ to $\sim 10^{-4}$ for $x=0.8$. Alternatively, it can be suggested that long-range magnetic coupling between the clusters diminishes with increasing V concentration, which is consistent with cluster-glass behavior of Fe_2VAl.[29] As shown in Fig. 2(b) a significant increase in magnetization value with increasing Cr content is observed at 7 K. All samples show nonsaturation, progressively more so as Cr concentration is reduced [see lower inset of Fig. 2(b)]. The slow approach to saturation along with negligible H_C and M_R values can be attributed to SPM-like behavior or distribution of finite magnetic clusters. The presence of FM component for the samples in the limit $x \to 1$ at 7 K is evidenced by the remanence magnetization and sharp increase in M at low fields. Significant increase in magnetization and opening up of hysteresis loop with Cr concentration are good indications of evolving FM correlations at lower temperature, even though SPM characteristics are dominant in $x=0$ alloy. It is also important to note that magnetization does not saturate even for an applied field of 15 kOe. Further, a strong support in favor of nonexistence of long-range ferromagnetic Fe state stems from the Mossbauer data, where a broad hyperfine field distribution, along with a paramagnetic component, has been observed and attributed to the presence of magnetic clusters in $Fe_2(Cr,V)Al$.[9,29] Besides, absence of spontaneous magnetization in Arrot plot for all the alloys indicates the presence of magnetic clusters at lower temperatures. These results indicate that the FM component at low temperature possibly stems from the strong intercluster interactions or distribution of cluster sizes with varying magnetic properties. These results cannot be explained on the basis of conventional theory proposed for ferromagnetism. In order to estimate various magnetic contributions in a system of N sites, with magnetic moment μ on each magnetic atom, the total magnetization as a function of field and temperature is given by[30]

$$M(H,T) = \left(\frac{N\mu_p}{V}\right)\left[P(p) + \int_1^\infty sn_s(p)\tanh\left(\frac{\mu_S H}{k_B T}\right)ds\right]. \tag{2}$$

The integral in Eq. (2) approximates a discrete sum over finite clusters, where $P(p)$ is percolation probability and $n_s(p)$ is cluster number distribution. However, a much simpler two-component magnetic (FM and SPM) combination yielded reasonably good fits to the 7 K data. At this temperature, magnetization data were fitted to the following expression:

$$M(H) = (1-\alpha)\left\{\frac{2M_{sf}}{\pi}\tan^{-1}\left[\frac{H \pm H_C}{H_C}\tan\left(\frac{\pi S}{2}\right)\right]\right\} + \alpha M_s L\left(\frac{\mu H}{k_B T}\right). \tag{3}$$

The first term in Eq. (3) is the function customarily used to fit FM hysteresis curve and the second part is SPM contribution to magnetization. The solid lines in the main panel of Fig. 2(b) correspond to the fits to the Eq. (3) and the parameters so obtained are listed in Table. I. Here S is the squareness of FM loop and is defined by $S=M_R/Ms_f$. On application of magnetic field most of the clusters can easily align along the field direction and result in saturation of magnetization at 7 K. However, the moment of clusters is less at low temperatures due to development of coupling between them, leading to nonsaturation of magnetization. Besides, the system could still contain PM or AFM matrix, resulting in nonsaturation even at higher fields. On the other hand, remarkable increases in magnetization values suggest that incorporation of Cr into the solid solution enhances intercluster interaction, eventually leading to conception of FM-like behavior as $x \to 1$. However, the absence of spontaneous magnetization indicates that the long-range FM order may not be realistic in these samples at 7 K. Instead, spatially confined FM clusters could exist. Comparison of magnetization curves at 300 and 7 K suggests the presence of a magnetic phase transition in the intermediate temperature range. Further, in depth investigation of temperature dependence of

TABLE I. Parameters extracted from SPM+PM fitting Eq. (1) and FM+SPM fitting Eq. (3) to the magnetization data at 300 and 7 K, respectively, and μ from fitting of Eq. (6) to MR data at these temperatures.

	300 K				7 K					
x	M_S (emu/g)	μ_{SPM} (μ_B)	$\chi_f(10^{-4})$ (emu/g Oe)	μ (from MR) (μ_B)	M_{Sf} (emu)	H_C (Oe)	M_R (emu)	M_S (emu/g)	μ_{SPM} (μ_B)	μ (MR) (μ_B)
0	0.05	5517	0.1	5517	03.0	0	0	05.3	10	08
0.2	0.06	4710	0.2	4623	09.9	7	0.3	10.5	94	89
0.4	0.27	4030	0.4	4011	14.6	7	0.4	14.9	266	265
0.6	0.32	3363	0.4		17.6	8	0.5	16.1	267	
0.8	0.57	2595	1.8	2259	27.8	9	0.8	27.2	706	781

magnetization can provide an insight on the nature of magnetic order.

C. Temperature dependence of magnetization

The zero-field-cooled (ZFC) and field-cooled (FC) magnetization curves as a function of temperature (T) under the external field of 100 Oe are shown in the Fig. 3. The magnetization shows history dependence with a bifurcation between ZFC and FC data at an irreversibility temperature (T_{irr}) for all the samples of present study. For the sample $x=0$ (see inset of Fig. 3), one can find that the M-T curves under ZFC and FC conditions do not overlap. The ZFC magnetization curve gradually increases on lowering the temperature from 300 K with a rapid increase below 10 K. A similar behavior has been observed in FC magnetization, while a bifurcation is seen between FC and ZFC curves at 240 K. On the other hand, for samples $x>0$, ZFC curve increases down to a certain temperature and then shows a downturn at lower temperatures. The FC curve invariably retraces the ZFC curve above magnetic transition temperature (T_S), but irreversibility in magnetization actually sets in at $T_{irr}<T_S$ (see Fig. 3). The T_S and M increase as the Cr concentration is increased. Thus, both M-H and M-T data appear to suggest that the volume fraction of FM component increases as Cr concentration is increased. Two possible reasons for this could be (i) the intercluster coupling becomes stronger either due to an increase in cluster size or a decrease in intercluster distance (ii) as Cr content is increased a secondary magnetic phase may be developing from the cluster-glass phase. The XRD results rule out the latter possibility as no secondary elemental/alloy phase is observed. However, from XRD patterns it is seen that increasing Cr content leads to site disorder, which in turn can have two inequivalent sites with different magnetic moments and can present a situation described in (i). As x increases, the cluster moment increases, but clusters coexist in a PM state. Hence, when the samples are cooled down to low temperatures in zero fields, the clusters enter a FM-like state due to stronger interaction effects, but the magnetization directions of the individual clusters are not aligned. When a small magnetic field is applied at 7 K, all the FM clusters cannot to rotate in the direction of applied field due to pinning force or small random anisotropy. Hence, even though the magnetization appears to saturate at higher applied fields, a linear component in M-H curve exists at 7 K.

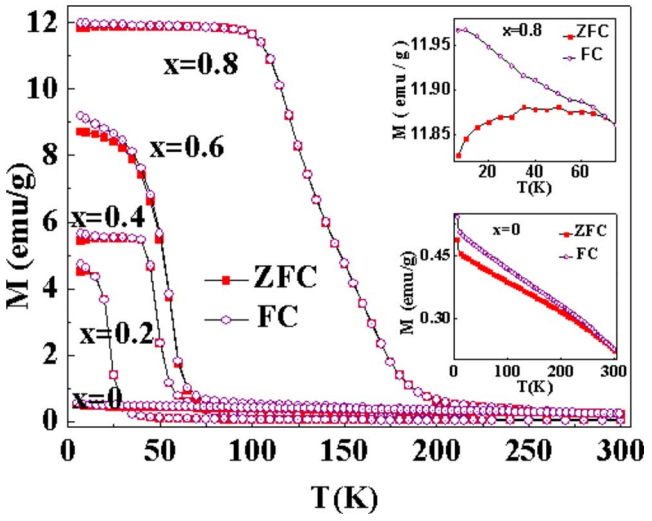

FIG. 3. (Color online) (Main panel) ZFC and FC ($H=100$ Oe) curves as a function of temperature of all the compositions. Insets: (upper) M-T curves for $x=0.8$ and (lower) for $x=0$ alloys are shown for better clarity.

The difference between FC and ZFC magnetization curves is usually attributed to the existence of spin-glass or cluster-glass phases. The cluster-glass-like features of concentrated magnetic systems originate from their magnetocrystalline anisotropy. An important point to be noted here is that FC magnetization continues to increase below T_{irr}, a typical feature of magnetic disorder. In canonical spin-glass systems, the FC shows a nearly constant value below T_{irr}. On the other hand due to the fact that cluster-glass exhibits short-range intracluster ferromagnetism below T_S, it may mimic some of the features of re-entrant spin-glass (RSG) system. Nevertheless, it may be noted that in several RSG systems, $T_{irr} \ll T_S$, whereas in cluster-glass systems, the irreversibility arises just below T_S as seen in Fig. 3. Although both T_S and T_{irr} increase with Cr substitution in the system, the difference between FC and ZFC curves is seen to decrease. We will address the genesis of this feature in subsequent paragraphs.

As pointed out in the earlier discussion, the irreversible magnetic behavior reflects the role of anisotropy in determining the shapes of the FC and ZFC curves below the ordering

temperature. Magnetic anisotropy aligns the spin in a preferred direction. Since no magnetic field is applied in ZFC process while cooling the sample through the ordering temperature, the spins are frozen in random directions for a polycrystalline sample. When a small magnetic field is applied at the lowest temperature, far below the magnetic transition temperature, the magnitude of resultant magnetization will depend on the anisotropy of the system. If the system is highly anisotropic, the small-applied field will not be sufficient to align the spins along field direction and hence the magnetization will be very small. On the other hand in FC process, the sample is cooled through its magnetic transition temperature in the presence of a magnetic field. Therefore the spins will be locked into a particular direction depending on the strength of the applied magnetic field as soon as the system is cooled below its ordering temperature. The FC magnetization will remain nearly constant if the anisotropy is low or increase with decreasing temperature for highly anisotropic materials. Therefore, during both ZFC and FC processes anisotropy field plays a crucial role in determining the magnetization under a given field strength.

Having convinced ourselves about the existence of anisotropy in the samples, we now turn our attention to investigate the effect of Cr concentration on anisotropy. To analyze the magnetic data we shall attempt to use the random anisotropy model (RAM) developed by earlier workers.[31] In the RAM formalism the magnetic ground state in a material is determined by the relative strength of a random anisotropy field that has lead to prediction of a variety of magnetic ground states. The strength of H is measured relative to a parameter H_s, where $H_s=\frac{H_r^4}{H_{ex}^3}$, with H_r and H_{ex} as the anisotropy and exchange fields, respectively. For low fields ($H<H_s$) one has a correlated spin glass, which has a large susceptibility and is equivalent to the Ahrony and Pytte[32] high-susceptibility phase. The RAM has been used previously to analyze magnetization data from cluster assembled films and amorphous alloys. Here, we extend it to a magnetically granular system. The random anisotropy causes the directions of the magnetization of locally correlated regions to vary. This regime is called the ferromagnet with wandering axis. In this regime, the magnetization approaches saturation as

$$M = M_0\left[1 - \frac{1}{15}\left(\frac{H_s}{H}\right)^{1/2}\right], \tag{4}$$

where M_0 is the saturation magnetization. For high fields ($H>H_{ex}$), all spins are virtually aligned with the field and there is only a slight tipping angle due to the anisotropy. In this regime, M is predicted to approach M_0 as

$$M = M_0\left[1 - \frac{1}{15}\left(\frac{H_r}{H + H_{ex}}\right)^2\right]. \tag{5}$$

The low-temperature M-H ($4 \le H \le 15$ kOe) data of all the samples are analyzed using Eq. (5) and shown in the Fig. 4, along with experimental data. An excellent agreement between the data and the RAM noted for all the samples at 7 K reinforces the assertion that the cluster-glass phase exists in these samples. The fit parameters extracted for all the samples are given in the Table II. It is seen that both the characteristic parameters H_r and H_{ex} decrease with Cr concentration. Relatively higher anisotropy field (H_r) and lower magnetization values result in an anisotropy constant (K_r) of $\sim 1.8\times 10^5$ erg/cm^3 for $x=0$, which compares well to the system that exhibits cluster-glass kind of behavior. Simultaneous decrease and increase in H_r and M values with increasing Cr content suggests development of a soft magnetic phase due to the reduction of anisotropy from 1.8×10^5 to 0.3×10^5 erg/cm^3. It is more likely that there are ferromagnetically correlated regions, the sizes of which are limited by the grain sizes, whose magnetization directions are pinned or frozen by random anisotropy. In other words at lower temperatures, where the strength of the random anisotropy is higher, the magnetization of correlated regions freezes into a cluster-glass state.

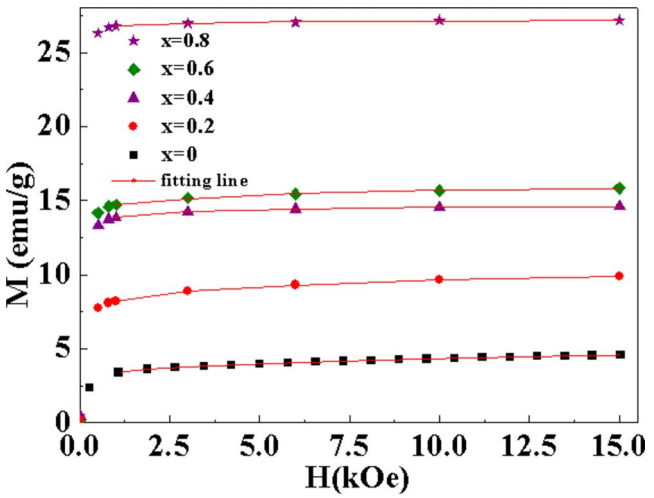

FIG. 4. (Color online) M-H plots of the alloys at 7 K along with the fits (solid line) to the Eq. (4).

As shown in Fig. 5 the temperature variation of inverse susceptibility for all the samples does not follow a simple Curie-Weiss (CW) law, instead a modified CW law $\chi=\chi_0+C/(T-\theta)$, where $C=N_A\mu_{eff}^2/(3k_B)$, N_A is Avogadro's number, μ_{eff} is the effective moment, μ_B is Bohr magneton, and θ is the Currie-Weiss temperature, fits well to the data in the limited temperature range above the transition temperature. However, on close observation it can be seen that χ^{-1} vs T plot obeys Curie-Weiss law in the limited temperature range with two different slopes. This suggests that the magnetic transition seen from M-T curves may be different from

TABLE II. Parameters from the RAM fitting Eq. (5) of M-H data at 7 K and from fitting of Eq. (6) of MR data.

x	M_0 (emu/g)	H_r (kOe)	H_{ex} (kOe)	H_S (kOe)	H_S (from MR data) (kOe)	$K_r(\times 10^5)$ (erg/cm^3)
0	05.47	69	29	9.29	9.87	1.88
0.2	10.61	33	18	2.03	2.82	1.63
0.4	14.96	16	15	0.19	0.19	1.19
0.6	16.04	11	09	0.20		0.88
0.8	27.22	3	06	0.003	0.02	0.41

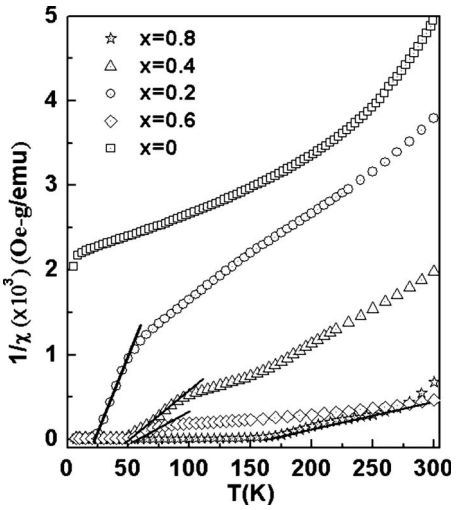

FIG. 5. Inverse magnetic susceptibility as a function of temperature. Solid lines represent fits to the modified Curie-Weiss law.

the conventional long-range magnetic order. It is worth noting that *M-H* curves at 300 K exhibit nonlinear behavior indicating SPM correlations rather pure paramagnetic behavior, which is consistent with χ^{-1} vs T data analysis. Slebarski *et al.*[19] reported that for a similar system, the Heusler alloy Fe_2TiSn, ferromagnetic correlation in the lattice due to atomic site disorder could have a remarkable effect on the magnetic moment. Their estimates of μ_{eff} and magnetic transition temperature (T_S) values from fits increase monotonically from $0.44\mu_B$/f.u. and 23 K for $x=0.2$ to $1.65\mu_B$/f.u. and 152 K for $x=0.8$, which are consistent with the experimentally reported values of $1.75\mu_B$/f.u. and 234 K for Fe_2CrAl.[20] Therefore from the present study it is clear that the magnetization and the transition temperature θ increase with increasing Cr content and consistent with the results reported earlier.[4,20] Although Zhang *et al.*[20] reported a PM-FM-like transition for $x=1$, present analysis along with earlier microscopic data suggests the presence of magnetic clusters with stronger coupling. However, a detailed critical behavior study will be valuable for ascertaining the nature of the transition.

From the magnetic data analysis it appears that Fe_2VAl behaves similar to a cluster glass. Substitution of Cr for V leads to FM-like behavior in Fe_2CrAl, probably due to intercluster coupling. We further suggest that the cluster-glass phase in Fe_2VAl is possibly developed due to the random anisotropy with the presence of V. However, FM-like order appears on Cr substitution because of strong intercluster coupling which in turn reduces the random anisotropy. This change in magnetic order can also affect the transport properties. Therefore electrical transport properties have been investigated.

D. Magnetoresistance

It is well established that magnetotransport behavior in granular materials is intimately related to the size, shape, and intercluster coupling. High MR values have been observed in the paramagnetic phase of the homogeneous $Au_{80}Fe_{20}$ alloys.[28] Another important parameter in obtaining higher MR values is the magnetic cluster size, which directly determines the spin-dependent scattering through the surface-to-volume ratio and intercluster distance. The predictions of the model agree with experiments suggesting that MR values depend on the size and shape of the magnetic clusters that are present in a nonmagnetic matrix. The important parameter that determines the resistance variation with field is $\langle \cos \varphi_{ij} \rangle$, where φ_{ij} is the angle between the axes of ferromagnetic entities over a distance of electronic mean-free path. For noninteracting particles if magnetization vectors are uncorrelated, the MR follows a quadratic dependence of reduced magnetization.[33] Any deviation from this law is indicative of the existence of correlations and therefore interaction effects between neighboring clusters should be taken in to account.[33] Kechrakos and Trohidou[34] investigated the combined effects of dipolar interactions and cluster size distribution on the MR of granular systems below the percolation threshold. They found that magnetostatic interactions and cluster size dispersion have opposite effects on MR value in these systems. Although the size dispersion alone causes enhancement of the MR, interactions lead to degrading effects. Further, their numerical study shows that the effect of dipolar interactions is amplified in the presence of a wide distribution of cluster sizes.

From the magnetization data we have observed that on Cr substitution in Fe_2VAl system, the coupling between the clusters gets enhanced. Therefore, the above predictions could be verified through the MR measurements on this series of samples. The MR, defined as $\Delta\rho/\rho = [\rho(H,T)-\rho(0,T)]/\rho(0,T)$, where $\rho(H,T)$ is the resistance of the sample under magnetic field H at temperature T, is shown in Figs. 6(a) and 6(b) as a function of H (up to 50 kOe) at 300 and 5 K, respectively. The MR is negative at all temperatures and fields for all the compositions of present study. The MR values in all samples remain well below 1% at 300 K, though the $x=0.8$ sample shows relatively larger MR value. At 5 K, a maximum value of 10% has been observed (at 50 kOe) in case of $x=0$ sample but it drops to 0.5% for $x=0.8$ sample. The low-temperature MR values and variation with H are similar to that observed in granular materials. For noninteracting magnetic clusters the MR scales approximately with the square of the H dependence of the magnetization. The MR is far from saturation even under 50 kOe, which indicates the importance of spin disorder contribution to the MR. A similar MR behavior has been reported in granular Co-Cu (Refs. 26–28) and cluster-glass Au-Fe alloys.[35] The MR is expressed as an even function $[\Delta\rho/\rho = -\mathrm{AF}(m)]$ of the reduced magnetization $m = M(H)/M_s$. Here, $M(H)$ is global magnetization, M_s is its saturation value, $F(m)$ is an even function of m, and prefactor A sets the overall magnitude of the MR. The function $F(m)$ was tried with a two-component function representing the sum of FM and a SPM component as implemented by Rubinstein *et al.*,[27] that seems to yield reasonably good fits, establishing the fact that the samples contain a distribution of clusters size ranging from SPM to FM

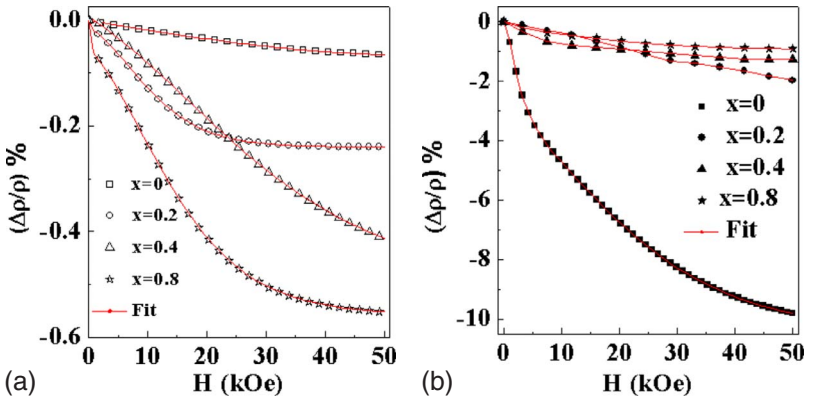

FIG. 6. (Color online) (a) Magnetoresistance as a function of applied field at 300 K. Solid lines represent fits to Eq. (6). (b) Magnetoresistance as a function of applied field at 5 K. Solid lines represent fits to the Eq. (6).

$$F(m) = \left[(1-\alpha)\left\{ \exp\left(-\frac{H}{H_S} \right) \right\} - \alpha L\left(\frac{\mu H}{k_B T} \right) \right]^2. \quad (6)$$

The first component of Eq. (6) is a function which vanishes when $H=0$ and saturates near $H=H_S$. It represents the progressive saturation of the FM clusters, whereas H_S is the saturation field and $(1-\alpha)$ is the FM fraction. The second component of Eq. (6) represents the field and temperature dependence of the SPM fraction of the sample. Here T is absolute temperature and μ is magnetic moment of the SPM cluster, which is a quantity proportional to the number of individual spins within the average SPM cluster. The solid lines through the data points shown in Figs. 6(a) and 6(b) are fits to Eq. (6). It is seen from the figure that the experimental data could be fitted well using a combination of FM and SPM terms. The parameters obtained from these fits are consistent with magnetization data (see Table I). The extracted parameters allow us to estimate the SPM (α) and FM fractions in the alloy. It can be seen from the table that all the samples exhibit SPM/PM character at 300 K with a large cluster moment: $5517\mu_B$ for $x=0$ which reduces to $2259\mu_B$ for $x=0.8$, suggesting a reduction in SPM cluster moment/size as the Cr concentration increased. At 5 K the $x=0$ sample exhibits similar behavior as that of granular alloys,[36] but substitution of Cr results in significant reduction of MR values probably due to development of intercluster interactions. This is reflected in simultaneous reduction of parameter "α" and enhancement of saturation magnetization (M_S). These results are consistent with magnetization data presented in this paper as well as reported results on Fe_2VAl and Fe_2CrAl alloys.[18,20] It is possible that the Fe_2VAl composition is a material with optimum number of SPM clusters to produce a large MR (10% at 5 K).

The temperature dependence of MR of all the samples is shown in Fig. 7. A dramatic reduction in MR has been observed in case of $x=0$, when temperature is raised to 300 K. For $x=0.4$ a maximum in MR (4%) has been observed at about 100 K, while for $x=0.8$ maximum (3%) is observed at 150 K, suggesting that as Cr concentration is increased, the MR values drop quite significantly, exhibiting a maximum value of MR near magnetic transition temperatures. In order to establish the relationship between SPM fraction and MR, the MR and α are plotted in the inset of Fig. 7 and from the figure it is clear that Cr content decreases α (i.e., increases FM correlations) and MR at 5 K. This experimental observation is in agreement with the theoretical predictions, where it was suggested that the dipolar interactions may lead to reduction of MR.[34] The coupling between the clusters becomes weaker as temperature is increased to a critical value where the spin disorder scattering dominates and larger values of MR can be noticed. This is the rationale behind the maximum observed in MR in the vicinity of magnetic transition temperature (see Fig. 7).

IV. DISCUSSIONS

Intermetallic Fe_3Al is a ferromagnetic compound having a DO_3 structure with a Curie temperature of ~770 K. Both Fe_2TMAl (TM: V, Cr) compositions have been derived from Fe_3Al by substituting V and Cr for iron. It is observed that the Curie temperature and magnetic moment decrease with increasing vanadium concentration and long-range FM order disappears in the vicinity of Fe_2VAl composition with a perfectly ordered $L2_1$ crystal structure, while Fe_2CrAl forms a B2 crystal structure with reduced magnetic moment and T_C

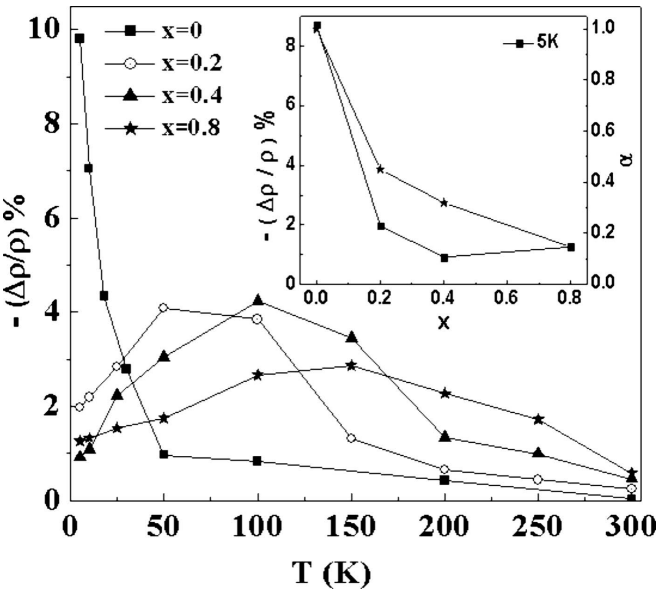

FIG. 7. Magnetoresistance (at 50 kOe magnetic field) as a function of temperature of all compositions. Inset: Variation of magnetoresistance and fractional coefficient of SPM component at 5 K with Cr concentration (x).

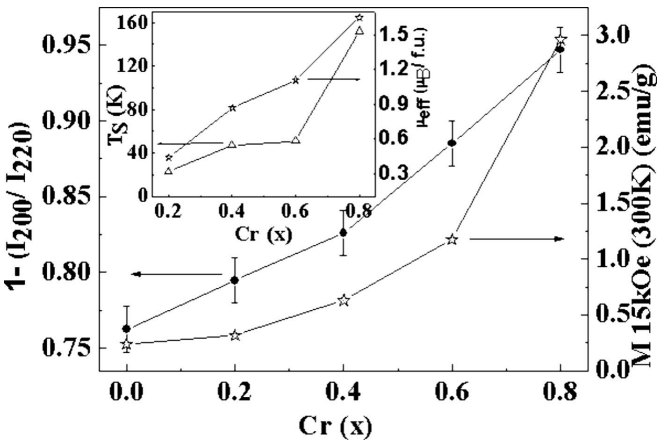

FIG. 8. Magnetization and the estimated site disorder parameter (XRD) as a function of Cr concentration. Inset: Variation of transition temperature and magnetic moment with Cr concentration.

but shows FM features below certain temperature (246 K). It was shown by earlier workers that the chemical and site disorders in these alloys could alter the magnetic properties significantly. Although all the alloys in the present study exhibit similar XRD patterns, altered lattice constants and significant changes in (200) superlattice reflection peak are observed, arising from atomic site disorder between Fe and Al due to incorporation of Cr atoms into the lattice. These site and chemical disorders may alter the magnetic moment and induce magnetic correlations in the system with increasing Cr concentration. The $L2_1$ structure is a superstructure for the B2 structure. For example, band-structure calculations showed Fe_2VAl to be nonmagnetic but the experimental results show a weakly magnetic state and this behavior is attributed to the presence of antisite defects. It is observed that effective magnetic moment of $x=0.8$ composition ($1.65\mu_B$/f.u.) is close to the value $1.67\mu_B$/f.u for Fe_2CrAl having B2 structure, as reported by Buschow and van Engen,[37] actually indicating the presence of atomic site disorder in the lattice for Cr-rich compositions. Magnetizations versus temperature curves (ZFC, FC) suggest the presence of magnetic disorder and a transition to a magnetically ordered state. Although the irreversibility in M-T curves at low fields has been observed in conventional ferromagnets well below T_C, it is generally attributed to the progressive stiffening of domain walls as the temperature is lowered through T_C to low temperatures. Indeed in all the samples investigated here that vary either in the degree of site disorder or composition, irreversibility in M-T curves is observed well below transition temperatures. But the M-T curves neither follow Bloch's law nor show the presence of spontaneous magnetization (Arrot's plot) below transition temperature. Therefore, above mechanism may not be relevant to the present case. Absence of spontaneous magnetization and presence of at least two magnetic components in M-H curves even below transition temperature indicate spatially confined FM, i.e., the clusters of FM order in the alloy. Further, features of long-range ferromagneticlike order develop from spatially confined cluster-glass-like state (Fe_2VAl), possibly due to the decrease in anisotropy constant from 1.8×10^5 to 0.32×10^5 with Cr content, which is evident from 7 K M-H curves [inset of Fig. 2(b)]. Now the most pertinent question is whether the site disorder can account for the change in magnetic properties observed in $Fe_2V_{1-x}Cr_xAl$ system. In order to verify this, site disorder parameter (estimated from XRD patterns) and magnetic parameters ($M_{15\ K}, T_S$) as a function of Cr concentration are plotted in Fig. 8, which show similar variations, indicating that site disorder plays a significant role. This observation is in agreement with earlier reports with different compositions.

On the other hand, it is well known that incorporation of early transition metals such as Cr and V into Fe-rich alloys rapidly decreases T_C and magnetic moment due to the AFM coupling between Fe and transition metals. In some cases these substitutions lead to a magnetically frustrated state due to the coexistence of FM and AFM heterogeneous regions in the sample.[36] Such materials exhibit a variety of magnetic characteristics such as re-entrant spin glass, cluster glass, or micromagnetic behaviors. Therefore, it is possible that the magnetic properties of $Fe_2V_{1-x}Cr_xAl$ alloy system could be assessed by the relative interaction strengths of Fe-Cr and Fe-V. From the present data it appears that the AFM interaction strength of Fe-V dominates over that of Fe-Cr, which is reflected in concentration dependence of anisotropy. At low temperatures this anisotropy grows sufficiently large that it severs many of the weak links holding rather tenacious infinite clusters together. The anisotropy then points these divided clusters along randomly preferred directions. But the "infinite cluster" FM state is not truly long range. The origin of these clusters with different magnetic moments is believed to arise from the site occupancy in crystal structure, as confirmed by previous theoretical and experimental observations. Using bimodal distribution of magnetic clusters, large MR can also be consistently explained, i.e., the moments of large particles will be more easily aligned than those of smaller ones at a given temperature. The large clusters are then responsible for the low-field variation of the MR and small ones for the slow approach. Therefore, the cluster sizes and the coupling between them dictate the variation of MR. As shown in the Fig. 7 the MR percentage at 5 K and paramagnetic fraction α values obtained from fit of Eq. (6) to the data follow same trend indicating a link between the clusters sizes and interactions to the MR behavior. The strong increase of MR with decreasing temperature is due to the increased tendency of alignment of the moments of the granules in the external field. This behavior is closely related to the magnetization. It is possible that, as a result of site disorder, spin clusters with larger moment are formed with increasing Cr concentration, while the coupling between the clusters is dramatically enhanced. This leads to cluster ordering, a feature essentially responsible for long-range FM-like behavior and reduced MR values.

The overall physical picture that emerges from the present investigation can be summarized as follows. Well above transition temperatures the system exhibits paramagnetic behavior and as temperature decreases many of the randomly positioned freely rotating spins build themselves into clusters which can then grow in size and rotate as a whole. A further reduction in temperature results not only in increasing the number of such cluster but also enhances interaction between

the clusters. Finally these large finite cluster moments probably begin aligning at some temperature, leading to a sudden increase in magnetization. As the Cr content increases the intercluster interaction strength increases and a ferromagneticlike order is observed. Therefore, we are tempted to suggest that Fe_2CrAl may be considered as system, which consists of densely packed magnetic clusters and shows soft-magnetlike properties as a result of interactions between clusters or clusters and the bulk matrix.

V. CONCLUSIONS

Structural, magnetic, and magnetotransport properties of $Fe_2V_{1-x}Cr_xAl$ ($x=0-0.8$) Heusler-type alloys have been investigated through room-temperature x-ray diffraction, low-temperature dc magnetization, and magnetoresistance measurements. From the detailed analysis of the magnetic field and temperature dependence of magnetization and magnetoresistance data, the following conclusions could be drawn:

(1) X-ray diffractograms confirm that all the alloys with composition $Fe_2V_{1-x}Cr_xAl$ ($x=0-0.8$) stabilize in Heusler $L2_1$ crystal structure with no sign of the presence of other phases, though increasing incorporation of Cr into the lattice promotes site disorder of Fe and Al.

(2) Magnetic and magnetoresistive properties show significant changes with Cr substitution. The magnetization data support the presence of superparamagnetic clusters at 300 K for all the compositions. However at 7 K the presence of FM-like behavior is evidenced by the remanence magnetization and sharp increase in M at low fields. In other words, at lower temperatures where the strength of the random anisotropy is higher, the magnetization of correlated regions freezes into a cluster-glass state. Anisotropy field is larger in $x=0$ sample and decreases with Cr concentration in the solid solution. Therefore, we suggest that alloy $x=0$ is in the cluster-glass phase developed possibly due to the random anisotropy (dipolar) with the presence of V. However, when the V atoms are replaced with Cr atoms it appears the AFM coupling reduces and as a result of this magnetic component increases to establish long-range order.

(3) Both magnetization and magnetoresistance show similar changes suggesting that Fe_2VAl composition is a material with optimum number of SPM clusters to produce a large MR (10% at 5 K). This magnetic cluster state transforms into a long-range ordered state when V is replaced with Cr and therefore Fe_2CrAl shows a soft ferromagnetlike behavior.

ACKNOWLEDGMENTS

The present work is partially supported by the Board of Research in Nuclear Sciences (BRNS), Department of Atomic Energy (DAE), Mumbai, India. Structural and low-temperature magnetoresistance measurements were performed with the support from DST/FIST Laboratory and the same is gratefully acknowledged.

*Corresponding author. FAX: +91-3222-255303; veeturi@phy.iitkgp.ernet.in

[1] R. A. de Groot, F. M. Mueller, P. G. van Engen, and K. H. J. Buschow, Phys. Rev. Lett. **50**, 2024 (1983); R. A. de Groot and K. H. J. Buschow, J. Magn. Magn. Mater. **54-57**, 1377 (1986).
[2] W. E. Pickett and J. S. Moodera, Phys. Today **54**(5),39 (2001).
[3] I. Zutic, J. Fabian, and S. Das Sharma, Rev. Mod. Phys. **76**, 323 (2004).
[4] E. Shreder, S. V. Streltsov, A. Svyazhin, A. Makhnev, V. V. Marchenkov, A. Lukoyanov, and H. W. Weber, J. Phys.: Condens. Matter **20**, 045212 (2008).
[5] Y. Nishino, H. Sumi, and U. Mizutani, Phys. Rev. B **71**, 094425 (2005).
[6] A. Slebarski, J. Goraus, J. Deniszczyk, and L. Skoczen, J. Phys.: Condens. Matter **18**, 10319 (2006).
[7] M. Kawakami, J. Magn. Magn. Mater. **128**, 284 (1993).
[8] D. E. Okpalugo, J. G. Booth, and C. A. Faunce, J. Phys. F: Met. Phys. **15**, 681 (1985).
[9] E. Popiel, M. Tuszynski, W. Zarek, and T. Rendecki, J. Less-Common Met. **146**, 127 (1989); Hyperfine Interact. **51**, 981 (1989).
[10] G. Y. Guo, G. A. Botton, and Y. Nishino, J. Phys.: Condens. Matter **10**, L119 (1998).
[11] R. Weht and W. E. Pickett, Phys. Rev. B **58**, 6855 (1998).
[12] A. Bansil, S. Kaprzyk, P. E. Mijnarends, and J. Tobola, Phys. Rev. B **60**, 13396 (1999).
[13] D. J. Singh and I. I. Mazin, Phys. Rev. B **57**, 14352 (1998).
[14] M. Tuszyński, W. Zarek, and E. S. Popiel, Hyperfine Interact. **59**, 369 (1990).
[15] S. M. Podgornykh, A. D. Suyazhin, E. I. Shreder, V. V. Marchenkov, and V. P. Dyakina, JETP **105**, 42 (2007).
[16] Y. Feng, M. V. Dobrotvorska, J. W. Anderegg, C. G. Olson, and D. W. Lynch, Phys. Rev. B **63**, 054419 (2001).
[17] C. S. Lue, J. H. Ross, C. F. Chang, and H. D. Yang, Phys. Rev. B **60**, R13941 (1999).
[18] M. Vasundhara, V. Srinivas, and V. V. Rao, Phys. Rev. B **77**, 224415 (2008).
[19] A. Slebarski, M. B. Maple, E. J. Freeman, C. Sirvent, D. Tworuszka, M. Orzechowska, A. Wrona, A. Jezierski, S. Chiuzbaian, and M. Neumann, Phys. Rev. B **62**, 3296 (2000).
[20] M. Zhang, E. Bruck, F. R. de Boer, and G. Wu, J. Magn. Magn. Mater. **283**, 409 (2004).
[21] E. I. Shreder, A. D. Svyazhin, A. A. Makhnev, A. N. Ignatenkov, L. D. Sairzyanova, and V. S. Gaviko, Phys. Met. Metallogr. **99**, 393 (2005).
[22] N. Lakshmi, K. Venugopalan, and J. Varma, Pramana, J. Phys. **59**, 531 (2002).
[23] E. Popiel, W. Zarek, and M. Tuszynski, Nukleonika **49**, s49 (2004).
[24] N. Lakshmi, R. K. Sharma and K. Venugopalan, Hyperfine Interact. **160**, 227 (2005).
[25] A. Kellou, N. E. Fenineche, T. Grosdidier, H. Aourag, and C. Coddet, J. Appl. Phys. **94**, 3292 (2003).
[26] A. E. Berkowitz, J. R. Mitchell, M. J. Carey, A. P. Young, S.

Zhang, F. E. Spada, F. T. Parker, A. Hutten, and G. Thomas, Phys. Rev. Lett. **68**, 3745 (1992); P. Allia, M. Knobel, P. Tiberto, and F. Vinai, Phys. Rev. B **52**, 15398 (1995).

[27] M. Rubinstein, V. G. Harris, B. N. Das, and N. C. Koon, Phys. Rev. B **50**, 12550 (1994).

[28] P. Allia, M. Coisson, J. Moya, V. Selvaggini, P. Tiberto, and F. Vinai, Phys. Rev. B **67**, 174412 (2003).

[29] M. Vasundhara, V. Srinivas, and V. V. Rao, Phys. Rev. B **78**, 064401 (2008).

[30] D. Stauffer, Phys. Rep. **54**, 1 (1979).

[31] E. M. Chudnovsky, W. M. Saslow, and R. A. Serota, Phys. Rev. B **33**, 251 (1986).

[32] A. Aharony and E. Pytte, Phys. Rev. Lett. **45**, 1583 (1980).

[33] J. Q. Xiao, J. S. Jiang, and C. L. Chien, Phys. Rev. Lett. **68**, 3749 (1992); M. El-Hilo, K. O'Grady, and R. W. Chantrell, J. Appl. Phys. **76**, 6811 (1994).

[34] D. Kechrakos and K. N. Trohidou, Phys. Rev. B **62**, 3941 (2000).

[35] U. Brux, T. Schneider, M. Acet, and E. F. Wassermann, Phys. Rev. B **52**, 3042 (1995).

[36] P. Allia, M. Coisson, and G. F. Durin, J. Appl. Phys. **91**, 5936 (2002); P. Allia, M. Coisson, J. Moya, V. Selvaggini, P. Tiberto, and F. Vinai, Phys. Rev. B **67**, 174412 (2003).

[37] K. H. J. Buschow and P. G. van Engen, J. Magn. Magn. Mater. **25**, 90 (1981).